Coercivity of isotropic nanocrystalline $Pr_{12}Fe_{82}B_6$ ribbons

Hong-wei Zhang, Chuan-bing Rong, Jian Zhang, Shao-ying Zhang, and Bao-gen Shen
State Key Laboratory of Magnetism, Institute of Physics and Centre for Condensed Matter Physics, Chinese Academy of Sciences, Beijing 100080, China

(Received 31 May 2002; revised manuscript received 9 August 2002; published 27 November 2002)

The magnetization reversal has been examined by the temperature dependence of the coercivity, the initial magnetization curve, minor hysteresis loops, and thermal activation in isotropic nanocrystalline Pr-Fe-B ribbons. The coercivity mechanism is found to vary with temperature. At 20 K, the coercivity is mainly determined by strong pinning (by random inhomogeneities); while at room temperature it is mainly controlled by the nucleation of domain and localized pinning at grain boundaries. The influence of the grain-boundary character on magnetic hardening and the temperature dependence of intergrain exchange coupling and anisotropy have been investigated to discuss the coercivity mechanism.

DOI: 10.1103/PhysRevB.66.184436 PACS number(s): 75.50.Ww, 75.60.Ej

I. INTRODUCTION

Many efforts have been made to investigate the magnetizing reversal process because the high intrinsic coercivity ${}_iH_c$ is the prerequisite for materials applied as permanent magnets (PM's). After $R_2Fe_{14}B$-type magnets were found, both nucleation and domain-wall pinning models were extensively studied to explain the high coercivity.[1–7] For isotropic magnets, the experimental investigation is usually conducted in terms of the followings (1) the temperature dependence of ${}_iH_c$, (2) the initial magnetization curve (thermally and dc demagnetized), (3) minor hysteresis loops, and (4) the analysis of thermal activation volume v.

Since intergrain exchange coupling (IGEC) in nanocrystalline PM's was pointed out,[8] many experimental attempts[9–13] have been made to make good calculating properties real.[12–17] At the present time, the experimental optimum maximum energy product $(BH)_{max}$ is far less than the ideal one. For example, the room-temperature optimum $(BH)_{max}$ is about 180 kJ/m^3 for nanocomposite melt-spun Pr-Fe-B-type ribbons.[9–11] Furthermore, for these isotropic ribbons the value of remanence $(\mu_0 M_r)$ is larger than 1 T, and the coercivity $(\mu_{0i}H_c)$ no more than 0.7 T. As the value of the coercivity is less than that of the remanence, enhanced coercivity becomes the key to improve energy product. Recently quasicoherent nucleation mode[18] and domain wall depinning[19] have been reported from a simulation of hard-soft composites. But the calculated coercivity[12–19] is usually several times larger than the experimental one. A large problem is the difficulty of simulating the real microstructure in a magnet. That is why it is important to experimentally determine the mechanism of coercivity. For simplicity, single-phase nanocrystalline PM is the suitable candidate for the investigation because IGEC exists.

II. THEORETICAL BASIS

IGEC can be examined by a Henkel plot which is based on the theory for a noninteraction system or uniform domain wall pinning as in Refs. 20 and 3.

$$M_d(H) = M_r(\infty) - 2M_r(H), \tag{1}$$

where the remanent magnetization $M_r(H)$ is acquired after the application and subsequent removal of a direct field H, $M_d(H)$ after dc saturation in one direction, and the subsequent application and removal of a direct field H in the reverse direction. $M_r(\infty)$ is denoted as M_r for convenience. Henkel first proposed that the deviation from this behavior in real systems was caused by the interactions between particles. The expression was given in Ref. 21 as follows:

$$\delta m(H) = [M_d(H) - M_r + 2M_r(H)]/M_r. \tag{2}$$

It is IGEC that makes an interaction domain possible in nanocrystalline PM's, as previously reported in Refs. 3 and 22. An interaction domain is composed of many grains. Thus, in nanocrystalline PM's, the coercivity mechanism may be different from that in traditional PM's with grain sizes in the micrometer scale.[10] That is why in this paper we first check IGEC using a Henkel plot in $Pr_{12}Fe_{82}B_6$ ribbons.

The temperature dependence of the coercivity can be expressed as[2,3,6]

$$H_c = \alpha_k \alpha_\varphi H_N - N_{eff} M_s, \tag{3}$$

where α_k, α_φ, and N_{eff} are microstructure parameters, and H_N is the nucleation field. Both nucleation and domain-wall pinning models can be explained by the equation. Due to the existence of IGEC, it is difficult to discuss the magnetization reversal in terms of pure pinning and/or nucleation models even in nanocrystalline single-phase PM's.[10] To explain the effect of IGEC on coercivity, Eq. (2) has been changed to[9]

$$H_c = \alpha_{ex} \alpha_k \alpha_\varphi H_N - N_{eff} M_s, \tag{4}$$

where α_{ex} takes into account the effect of the exchange coupling between neighboring grains. In consideration of grain size d, the above equations have been suggested to be[22]

$$H_c = \frac{\alpha_k \alpha_\varphi}{1 + 6\beta_k l_{ex}/d} H_N - \frac{N_{eff}}{1 + 6\beta_s l_{ex}/d} M_s, \tag{5}$$

where l_{ex} is the ferromagnetic exchange length, and β_k and β_s depend on the nature of the grains boundary concerning anisotropy and stray field, respectively. Up to now, no way has been found to determine the experimental values of α_{ex},

β_k, and β_s, so it is difficult to analyze the magnetic reversal mechanism only according to the temperature dependence of the coercivity.

Hysteresis results from the existence of energy barriers. Thermal activation enables a magnetization irreversible reversal, which is a little different from the external applied field. Thus the thermal activation volume v is expected to give some information on the coercivity mechanism. Since the use of Barbier plot was emphasized by Wohlfarth,[23] the relationship between coercivity and v has been revised as[24]

$$\lg_i H_c = \lg v^{-1} + b(T), \tag{6}$$

where $b(T)$ is a constant at a given temperature, which is expected to be useful in discussing the mechanism of magnetization reversal. For strong domain-wall pinning and domain-wall unpinning, the coercivity in the above equation is related to the product of the range of interaction l and the maximum pinning force f due to a pin.[25,26] In this work, the magnetization behavior is extensively investigated in order to clarify the magnetization reversal mechanism in isotropic nanocrystalline $Pr_{12}Fe_{82}B_6$ ribbons.

III. EXPERIMENTS

Isotropic nanocrystalline $Pr_{12}Fe_{82}B_6$ ribbons were prepared as described in Ref. 9. Only a $Pr_2Fe_{14}B$ phase was found in the ribbons by TEM and x-ray diffraction, and the grain size of about 20 nm was checked by TEM.[27] The magnetic measurements were carried out using a superconducting quantum interference device with a maximum field $\mu_0 H$ of 6.5 T applied along the longitudinal direction of the ribbons. In such a case, the demagnetization factor could be neglected. The minor loop was measured by one cycle between an applied field H and $-H$. The magnetic viscosity was measured at temperatures ranging from 20 K to room temperature (RT). The magnetic viscosity constant was obtained by fitting the time dependence of the magnetization, and the thermal activation volume v by the method as reported in Ref. 23.

IV. RESULTS AND DISCUSSION

A nonuniform distribution of strain, which can influence the coercivity by its effective magnetoanisotropy K_s, can be formed in the melt-spun ribbons. Usually, K_s is proportional to the product of the magnetostriction constant λ and the stress σ. It is difficult to determine the value of λ in the ribbons. However, we can give an estimation as follows: supposing K_s is 1 MJ/m^3 (the same order of magnetocrystalline anisotropy K_1) and λ is 100 ppm, σ will be about 10^5 kg/cm^2. The value of σ is too large to be reasonable. In other words, the distribution of stress plays an important role in coercivity for magnetic soft materials.

Figure 1 shows the Henkel plot obtained according to Eq. (2). As mentioned in Refs. 1, 3, and 28, a strong interaction is exhibited in the sample. Compared with the observation of the interaction domain,[3,22] it is clear that the interaction is mainly contributed by IGEC. As shown in Fig. 1, the intergrain exchange coupling grows slightly with a drop in the temperature. The coercivity mechanism of uniform domain wall pinning can be excluded due to the existence of nonzero $\delta m(H)$.[3]

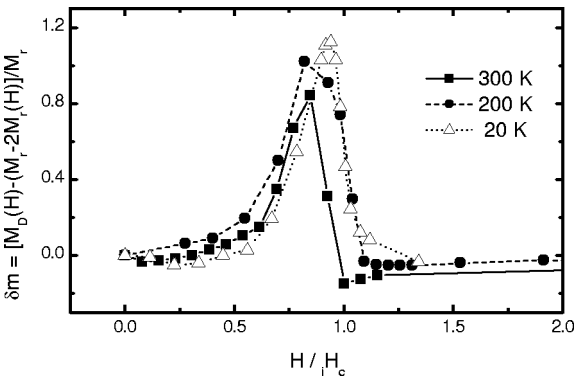

FIG. 1. The measuring Henkel plot of the ribbons.

Plots of the coercivity and remanence versus the maximum applied field are shown in Figs. 2(a) and 2(b), respectively. Figure 3 shows the initial magnetization curves for thermal demagnetized sample. At RT, the field dependence of the coercivity can be approximately predicted by a nucleation model.[1–3] The difference between positive and negative magnetizing directions is caused by inhomogeneous domain-wall pinning, since uniform pinning is already excluded. A similar behavior is also observed in the variation of remanence with field [shown in Fig. 2(b)]. The coercivity seems to be mainly controlled by nucleation, while domain-wall inhomogeneous pinning cannot be neglected at the same time.[1–3,6,7] An eclectic explanation is that both pinning and nucleation determine the magnetization reversal at RT. The deduction can also be confirmed by the initial magnetization curve, as shown in Fig. 3. Traditionally, domain walls move

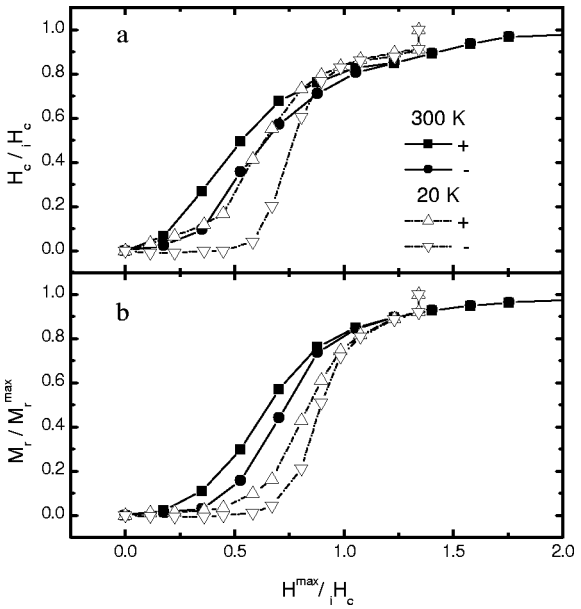

FIG. 2. Coercivity and remanence vs the maximum applied field of the ribbons, the coercivity, and the remanence obtained from the minor loop. + represents the values obtained in the second quadrant, and − those in the fourth quadrant.

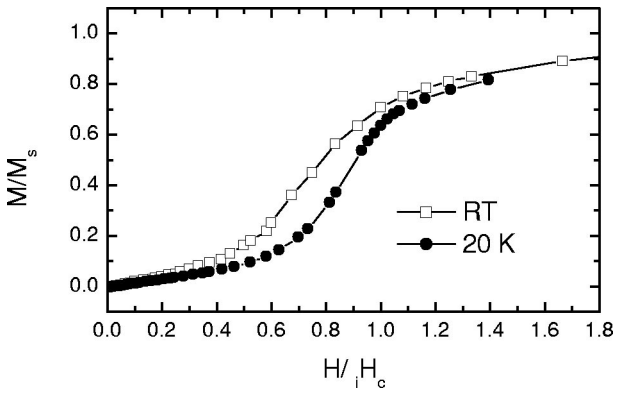

FIG. 3. The initial magnetization curves for the thermal demagnetized sample.

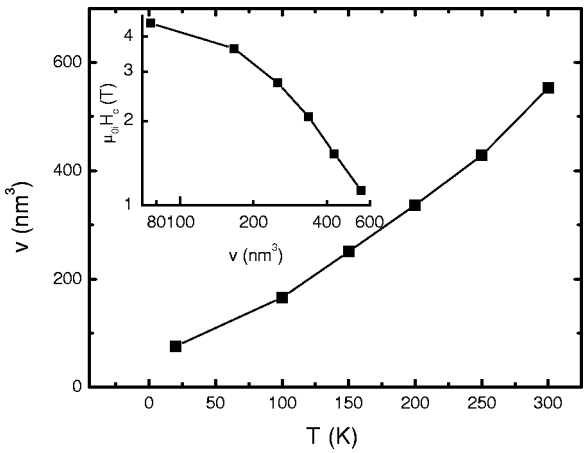

FIG. 4. The dependence of the thermal activation volume v on the temperature. The inset is the plot of $_iH_c$ vs v.

easily inside grains; therefore large susceptibilities are expected for nucleation. Domain walls are pinned; therefore there are low virgin susceptibilities for pinning. A moderate case is presented in Fig. 3, which can be explained by the fact that an interaction domain wall can easily move inside grains and be locally pinned at grain boundaries in the interaction domain. However, at 20 K, the coercivity mechanism is mainly controlled by domain-wall pinning, as shown in Fig. 2. Larger differences of the variation of coercivity and remanence with field between positive and negative magnetizing directions are observed compared with that at RT. This means that the inhomogeneous pinning effect is strengthened. A similar result can be found in the initial magnetization curve in Fig. 3. Thus the magnetization reversal at 20 K is chiefly caused by the domain-wall inhomogeneous pinning. It is interesting that the mechanism of magnetization reversal changes with temperature.

A nanocrystalline PM exhibits characteristics of an interaction domain. As cited in Ref. 8, the neighboring grains need to be crystallographically coherent and exchange coupled through the boundaries. When a domain is composed of only one nanoscaled grain, there will be a very large domain-wall energy, except in a case without IGEC (e.g., magnetic grains are separated by a nonmagnetic intergrain phase[29]). Thus an interaction domain showing a multigrain in a domain is expected, which is quite different from traditional PM's characterized by a single domain grain or a multidomain grain. There are great numbers of nucleation and/or pinning center related imperfections in a grain boundary, so the inhomogeneity inevitably exists in a multigrain domain for the ribbons. Let us consider the effect of the grain-boundary character on the demagnetization behavior. The width of the intergrain inhomogeneity is 3–5 nm for this kind of ribbons.[30] This means that r_0 is approximately equal to the Bloch wall width δ_B, where r_0 represents the width of imperfection layer δ_B as $\pi\sqrt{A/K}$ (A is the exchange coupling constant and K the magnetocrystalline anisotropy constant). Because IGEC forces the magnetization to deviate somewhat from the local easy axis and a multigrain domain is formed, the following equations can be approximately used to discuss the nucleation field and the pinning field at grain boundaries for the ribbons. The nucleation of a reversed domain wall gives an expression for the coercivity in the form of Eq. (3) as[2]

$$\alpha_k^{nuc}(T) \approx \delta_B / \pi r_0 . \tag{7}$$

In contrast, the pinning of the domain wall is

$$\alpha_k^{pin}(T) = \frac{1}{3\sqrt{3}} \frac{\pi r_0}{\delta_B} \left(\frac{A}{A'} - \frac{K'}{K} \right) \propto \frac{\pi r_0}{\delta_B} \tag{8}$$

for $r_0 < \delta_B$, and

$$\alpha_k^{pin}(T) \approx 2\delta_B / 3\pi r_0 \tag{9}$$

for $r_0 > \delta_B$. In order to determine an approximate value of α_k^{pin} for $r_0 \approx \delta_B$, the crossover point of the two extreme cases is considered. Kronmuller *et al.*[2] considered the case of $A = A'$ and $K \gg K'$, and found that the maximum α_k^{pin} for pinning is 0.3. Furthermore, Liu *et al.*[7] performed complementary work for the case of $A > A'$, and obtained that the maximum α_k^{pin} for pinning may exceed 0.3. Recently, $A > A'$ was discussed by continuum and layer-resolved calculations,[13] and supported by experiments in nanocrystalline PM's.[31] This means that α_k^{pin} is probably equal to α_k^{nuc} for $r_0 \approx \delta_B$. In other words, the nucleation field is approximately equal to the pinning field in this case. With a drop of the temperature, δ_B falls because of the rapid rise of K. Thus the value of r_0 / δ_B grows with the drop of temperature. Comparing the nucleation field [as in Eq. (7)] with the pinning one [Eq. (9)], the lower coercivity given in Eq. (9) will truly occur at a low temperature. So, in this experiment, the magnetization reversal mechanism changes from a mixture of pinning and nucleation at RT to main pinning at 20 K. This is very consistent with the results obtained from Figs. 2 and 3.

Figure 4 shows the dependence of the thermal activation volume v on the temperature. v, comparable to the volume of the inner part (perfection) of a small grain, can be explained as the domain-wall jumping through the inner part of small grain at RT. v drops rapidly with falling temperature. At low temperature, it seems that v represents the volume covered by a single jump between pinning centers in a grain boundary for a domain wall. The inset of Fig. 4 shows the

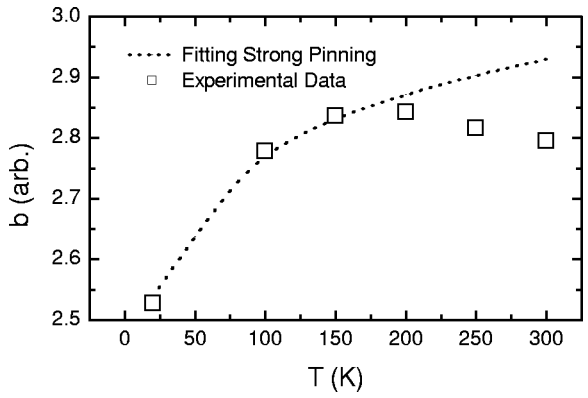

FIG. 5. The temperature dependence of *b*.

plot of ${}_iH_c$ versus v. The relation between ${}_iH_c$ and v was discussed in terms of strong pinning, weak pinning, unpinning, and single domain particles in Ref. 24. The relations cannot fit the experimental one at the temperature varying from 20 K to RT.

By using the experimental values of $H_c(T)$ and $v(T)$, $b(T)$ is directly obtained according to Eq. (6), and shown in Fig. 5. As given in Ref. 24, the expression for $b(T)$ is very complicated. For example, $b(T)=lg\{(75kT/4M_s)[(4fl/75kT)^{2/3}-1]\}$ for a strong pinning model.[24] Fortunately, as $(4fl/75kT)^{2/3} \gg 1$,[3,24] $b(T) \simeq lg[(4fl)^{2/3}(75kT)^{1/3}/4M_s]$. In a temperature range between 20 K and RT, the variation of kT is much faster than that of M_s and fl.[3] Thus, under the approximation of M_s and fl being constant, the temperature dependence of $b(T)$ can be discussed. The low-temperature part of $b(T)$ can be approximately fitted by a strong pinning model. When the temperature rises to RT, the strong pinning model cannot be used to explain what happens in the ribbons. It seems that there is a transition to coercivity mechanism. The high-temperature part of $b(T)$ is somewhat similar to that reported in Ref. 32, in which the coercivity is mainly controlled by an inhomogeneous pinning of nucleated type rather than by pure nucleation or a strong pinning model. Thus, at RT, some energy barriers can be overcome by thermal activation and nucleation is formed. The nucleation leads to a magnetization reversal of the inner part of a grain, but the nucleated domain wall is pinned at the grain boundary. This produces a large v comparable to the volume of the inner part of a small grain (as shown in Fig. 4). However, at low temperature, only some low energy barriers may be activated because the anisotropy of the matrix is strongly increased. In this case, even though nucleation can take place at a site in the grain boundary, it remains pinned at other centers in the same grain boundary.[6] It is better to take the small v as the volume covered by a jump between pinning centers in the same boundary. Therefore, the magnetic hardening mainly results from the nucleation of domain and localized pinning at grain boundaries for the ribbons at RT, and strong pinning at 20 K.

V. CONCLUSION

IGEC, which leads to a multigrain domain structure, is found in nanocrystalline isotropic $Pr_{12}Fe_{82}B_6$ ribbons using a Henkel plot. A nucleation field as well as a pinning field are analyzed considering the ratio of the imperfection layer width to δ_B. As the anisotropy increases quickly with a drop in the temperature, the observed demagnetization behavior is explained by an inhomogeneous pinning of nucleated type at RT and by a random strong pinning at 20 K. The magnetization reversal mechanism is further verified by the temperature dependence of the thermal activation volume.

ACKNOWLEDGMENTS

The work was supported by the State Key Project of Fundamental Research and the National Science Foundation of China. Our thanks are due to Professor Kronmuller and Dr. Goll for the provision of the melt-spun ribbons used in this work.

[1] F. E. Pinkerton and D. J. Van Wingerden, J. Appl. Phys. **60**, 3685 (1986).
[2] H. Kronmulller, K. D. Durst, and M. Sagawa, J. Magn. Magn. Mater. **74**, 291 (1988).
[3] G. C. Hadjipanayis and A. Kim, J. Appl. Phys. **63**, 3310 (1988).
[4] D. Givord, O. Lu, M. F. Rossignol, P. Tenaud, and T. Viadieu, J. Magn. Magn. Mater. **83**, 183 (1990).
[5] D. C. Crew, P. G. McCormick, and R. Street, J. Appl. Phys. **86**, 3278 (1999).
[6] K. H. J. Buschow, Rep. Prog. Phys. **54**, 1123 (1991).
[7] J. F. Liu, H. L. Luo, and J. Wan, J. Phys. D **25**, 1238 (1992).
[8] E. F. Kneller and R. Hawig, IEEE Trans. Magn. **27**, 3588 (1991).
[9] D. Goll, M. Seeger, and H. Kronmuller, J. Magn. Magn. Mater. **185**, 49 (1998).
[10] G. C. Hadjipanayis, J. Magn. Magn. Mater. **200**, 373 (1999).
[11] X. Y. Zhang, Y. Guan, L. Yang, and J. W. Zhang, Appl. Phys. Lett. **79**, 2426 (2001).
[12] E. E. Fullerton, J. S. Jiang, M. Crimsditch, C. H. Sowers, and S. D. Bader, Phys. Rev. B **58**, 12 193 (1998).
[13] R. Skomski, H. Zeng, and D. J. Sellmyer, IEEE Trans. Magn. **37**, 2549 (2001).
[14] R. Skomski and J. M. D. Coey, Phys. Rev. B **48**, 15 812 (1993).
[15] R. Fischer and H. Kronmuller, Phys. Rev. B **54**, 7284 (1996).
[16] J. Fidler and T. Schrefl, J. Magn. Magn. Mater. **203**, 28 (1999).
[17] M. K. Griffiths, J. E. L. Bishop, J. W. Tucker, and H. A. Davies, J. Magn. Magn. Mater. **183**, 49 (1998); **234**, 331 (2001).
[18] R. Skomski, J. P. Liu, and D. J. Sellmyer, Phys. Rev. B **60**, 7359 (1999).
[19] S. T. Chui and Y. Yu, Phys. Rev. B **63**, 140419(R) (2001).
[20] E. P. Wohlfarth, J. Appl. Phys. **29**, 595 (1958).
[21] P. E. Kelly, K. O. Grady, P. I. Mayo, and R. W. Chantrell, IEEE Trans. Magn. **25**, 3881 (1989).
[22] H. W. Zhang, Z. G. Sun, S. Y. Zhang, B. S. Han, B. G. Shen, I. C. Tung, and T. S. Chin, Phys. Rev. B **60**, 64 (1999).

[23] E. P. Wohlfarth, J. Phys. F: Met. Phys. **14**, L155 (1984).
[24] J. F. Liu and H. L. Luo, J. Magn. Magn. Mater. **94**, 43 (1991).
[25] P. Gaunt and C. K. Mylvaganam, Philos. Mag. B **44**, 569 (1981).
[26] U. S. Ram, D. Ng, and P. Gaunt, J. Magn. Magn. Mater. **50**, 193 (1985).
[27] D. Goll, Ph D. thesis, Max-Planck-Institut, Stuttgart, 2001.
[28] V. Basso and G. Bertotti, IEEE Trans. Magn. **30**, 64 (1994).
[29] E. Girt, K. M. Krishnan, G. Thomas, and Z. Altounian, Appl. Phys. Lett. **76**, 1746 (2000).
[30] A. Zern, Ph D. thesis, Max-Planck-Institut, Stuttgart, 1999.
[31] X. Y. Zhang, Y. Guan, and J. W. Zhang, Appl. Phys. Lett. **80**, 1966 (2002).
[32] H. W. Zhang, S. Y. Zhang, and B. G. Shen, Phys. Rev. B **62**, 8642 (2000).